Borrelia burgdorferi peptidoglycan is a persistent antigen in patients with Lyme arthritis

Brandon L. Jutras[a,b,c,1], Robert B. Lochhead[d,2], Zachary A. Kloos[a,e], Jacob Biboy[f,g], Klemen Strle[d], Carmen J. Booth[h], Sander K. Govers[a,b], Joe Gray[i], Peter Schumann[j], Waldemar Vollmer[f,g], Linda K. Bockenstedt[k], Allen C. Steere[d], and Christine Jacobs-Wagner[a,b,c,l,3]

[a]Microbial Sciences Institute, Yale University, West Haven, CT 06516; [b]Department of Molecular, Cellular, and Developmental Biology, Yale University, New Haven, CT 06511; [c]Howard Hughes Medical Institute, Yale University, West Haven, CT 06516; [d]Center for Immunology and Inflammatory Diseases, Massachusetts General Hospital and Harvard Medical School, Boston, MA 02114; [e]Microbiology Program, Yale School of Medicine, New Haven, CT 06510; [f]Centre for Bacterial Cell Biology, Newcastle University, NE2 4AX Newcastle upon Tyne, United Kingdom; [g]Institute for Cell and Molecular Biosciences, Newcastle University, NE2 4AX Newcastle upon Tyne, United Kingdom; [h]Department of Comparative Medicine, Yale School of Medicine, New Haven, CT 06510; [i]Institute for Cell and Molecular Biosciences, Newcastle University, NE2 4AX Newcastle upon Tyne, United Kingdom; [j]Leibniz Institute, Deutsche Sammlung von Mikroorganismen und Zellkulturen GmbH, 38124 Braunschweig, Germany; [k]Section of Rheumatology, Department of Internal Medicine, Yale School of Medicine, New Haven, CT 06510; and [l]Department of Microbial Pathogenesis, Yale School of Medicine, New Haven, CT 06510

Contributed by Christine Jacobs-Wagner, May 11, 2019 (sent for review March 14, 2019; reviewed by Thomas G. Bernhardt and Justin D. Radolf)

Lyme disease is a multisystem disorder caused by the spirochete *Borrelia burgdorferi*. A common late-stage complication of this disease is oligoarticular arthritis, often involving the knee. In ∼10% of cases, arthritis persists after appropriate antibiotic treatment, leading to a proliferative synovitis typical of chronic inflammatory arthritides. Here, we provide evidence that peptidoglycan (PG), a major component of the *B. burgdorferi* cell envelope, may contribute to the development and persistence of Lyme arthritis (LA). We show that *B. burgdorferi* has a chemically atypical PG (PG^{Bb}) that is not recycled during cell-wall turnover. Instead, this pathogen sheds PG^{Bb} fragments into its environment during growth. Patients with LA mount a specific immunoglobulin G response against PG^{Bb}, which is significantly higher in the synovial fluid than in the serum of the same patient. We also detect PG^{Bb} in 94% of synovial fluid samples (32 of 34) from patients with LA, many of whom had undergone oral and intravenous antibiotic treatment. These same synovial fluid samples contain proinflammatory cytokines, similar to those produced by human peripheral blood mononuclear cells stimulated with PG^{Bb}. In addition, systemic administration of PG^{Bb} in BALB/c mice elicits acute arthritis. Altogether, our study identifies PG^{Bb} as a likely contributor to inflammatory responses in LA. Persistence of this antigen in the joint may contribute to synovitis after antibiotics eradicate the pathogen. Furthermore, our finding that *B. burgdorferi* sheds immunogenic PG^{Bb} fragments during growth suggests a potential role for PG^{Bb} in the immunopathogenesis of other Lyme disease manifestations.

Lyme disease | arthritis | peptidoglycan | *Borrelia burgdorferi* | inflammation

Lyme disease, caused by the spirochete *Borrelia burgdorferi*, is the most prevalent tick-borne human disease in temperate regions of the Northern hemisphere (1). Clinical manifestations of this disease are highly variable and can involve multiple organ systems at different times (2). Infection in humans is often heralded by a skin lesion (known as erythema migrans) at the site of the tick bite. If left untreated, the infection can disseminate to other tissues (e.g., skin, heart, central nervous system, joints) and give rise to additional skin lesions, carditis, neurological disorders, or arthritis (3–5). These clinical outcomes are thought to result from host immune responses to *B. burgdorferi* or *B. burgdorferi*-derived components (6).

Arthritis is the most common late-stage clinical manifestation of Lyme disease in the United States and is often characterized by inflammation of one or more large joints (typically the knee), which are one of the sites the spirochetes frequently infiltrate (6). In ∼10% of cases, an inflammatory proliferative synovitis persists despite 2–3 mo of oral and intravenous (IV) antibiotic therapy and apparent absence of viable organisms in the synovial fluid and adjacent tissues (5, 7, 8). Development of autoimmunity is thought to contribute to the persistence of Lyme arthritis (LA), and recent studies have identified four autoantigens as targets of autoreactive T and B cell responses in patients with postinfectious LA (9–13). It has also been proposed that *B. burgdorferi*-derived components may persist after initial infection and serve as immunogens, contributing to inappropriate inflammation long after the spirochetes have been killed (14). However, such persistent immunogens have yet to be identified.

B. burgdorferi does not produce lipopolysaccharides (endotoxin), and its genome does not appear to encode effectors that might act as toxins (15, 16). Therefore, most studies to date have focused on surface-exposed lipoproteins anchored in the outer membrane of *B. burgdorferi*. These lipoproteins play important roles in various aspects of tick colonization, mammalian infection, and host immune evasion and response (17–19). Comparatively, the peptidoglycan (PG), an essential component of bacterial cell envelopes,

Significance

Lyme disease, caused by the spirochete *Borrelia burgdorferi*, is the most common vector-borne disease in North America. If early infection is untreated, it can result in late-stage manifestations, including arthritis. Although antibiotics are generally effective at all stages of the disease, arthritis may persist in some patients for months to several years despite oral and intravenous antibiotic treatment. Excessive, dysregulated host immune responses are thought to play an important role in this outcome, but the underlying mechanisms are not completely understood. This study identifies the *B. burgdorferi* peptidoglycan, a major component of the cell wall, as an immunogen likely to contribute to inflammation during infection and in cases of postinfectious Lyme arthritis.

Author contributions: B.L.J. and C.J.-W. designed research; B.L.J., R.B.L., Z.A.K., J.B., K.S., C.J.B., J.G., P.S., W.V., L.K.B., and A.C.S. performed research; B.L.J., R.B.L., Z.A.K., S.K.G., and W.V. analyzed data; and B.L.J., Z.A.K., and C.J.-W. wrote the paper with assistance from all authors.

Reviewers: T.G.B., Harvard Medical School; and J.D.R., University of Connecticut Health Sciences Center.

The authors declare no conflict of interest.

[1]Present address: Fralin Life Sciences Institute, Department of Biochemistry, College of Agriculture and Life Sciences, Virginia Tech, Blacksburg, VA 24061.

[2]Present address: Department of Microbiology and Immunology, Medical College of Wisconsin, Milwaukee, WI 53226.

[3]To whom correspondence may be addressed. Email: christine.jacobs-wagner@yale.edu.

This article contains supporting information online at www.pnas.org/lookup/suppl/doi:10.1073/pnas.1904170116/-/DCSupplemental.

has received very little attention. The PG, which is made of glycan strands cross-linked by short peptides, forms a polymeric meshwork around the cytoplasmic membrane and provides resistance against intracellular osmotic pressure (20, 21). PG is also a microbe-associated molecular pattern that can stimulate innate immune pathways in animals, resulting in inflammation (22). PG from Gram-positive bacteria administered intraarticularly or systemically can induce acute arthritis in mice and rats (23–29). NOD2, an innate immunity protein recognizing a PG moiety, has been implicated in proinflammatory cytokine production and immune tolerance during *B. burgdorferi* infection in mice (30, 31). Furthermore, a 1990 report has shown that *B. burgdorferi* PG (PG^{Bb}) stimulates interleukin 1 (IL-1) production in macrophages in vitro and that intradermal injection of PG^{Bb} in human volunteers results in skin reactions characteristic of inflammation (32). Despite these observations, a potential role for PG^{Bb} in *B. burgdorferi* pathogenesis has not been directly examined.

In diderm bacteria, including *B. burgdorferi*, the outer membrane shields the PG meshwork from the external environment. Exposure of PG^{Bb} to the host immune system may, however, still be significant for two reasons. First, spirochete death, which occurs during early stages of transmission and dissemination (33), may result in PG^{Bb} exposure to host immune cells. Second, sequence homology analyses predict that *B. burgdorferi* lacks a PG recycling pathway (34). Absence of PG recycling suggests that large amounts of PG fragments (known as muropeptides) may be released into the host environment during spirochetal growth. Bacteria degrade ∼40–50% of their PG per generation, as part of the normal PG remodeling process required for cell wall expansion (34–36). In Gram-negative/diderm bacteria, the vast majority of muropeptides produced during normal PG turnover are typically recycled. During this process, muropeptides are transported into the cytoplasm by an inner membrane permease (AmpG), processed by PG recycling proteins (e.g., AmpD and LdcA), and reincorporated into the PG biosynthetic pathway for reuse (*SI Appendix*, Fig. S1*A*) (34). Bacterial mutants that lack AmpG shed a large amount of muropeptides into their environment during growth (*SI Appendix*, Fig. S1*B*) (36–39). The apparent absence of a canonical muropeptide recycling pathway in *B. burgdorferi* suggests the possibility that muropeptides produced during normal PG turnover may be released into the extracellular milieu where the host immune system would be able to detect them. These considerations motivated us to test the hypothesis that PG^{Bb} is an antigen contributing to proinflammatory responses during the infectious and postinfectious phases of LA.

Results

***B. burgdorferi* PG Has an Unusual Chemical Composition.** We first characterized the chemical composition and architecture of purified PG^{Bb}. Liquid chromatography and mass spectrometry (LC-MS) analysis of cellosyl-digested PG revealed several unusual features (Fig. 1*A* and *SI Appendix*, Table S1). For instance, whereas the sugar backbone of the PG^{Bb} is made up of alternating *N*-acetylglucosamine (Glc*N*Ac) and *N*-acetylmuramic acid (Mur*N*Ac), similar to other bacterial PGs, we also observed the occasional presence of an *N*-acetylhexosamine (Hex*N*Ac) linked to Glc*N*Ac (Fig. 1*A*). To our knowledge, such a modification has not been reported in any other PGs characterized to date. Another feature of the PG^{Bb} was the presence of L-ornithine (L-Orn) linked to a single glycine (Fig. 1*A* and *SI Appendix*, Table S1), which is congruent with an earlier chemical amino acid analysis (32). The presence of L-Orn has been reported in other spirochetes (40). It is, otherwise, a rare deviation from the typical PG dichotomy in the bacterial domain (41), which generally features a diaminopimelic acid (DAP) or lysine (Lys) at the third amino acid position of the stem peptide. We confirmed the presence of L-Orn in PG^{Bb} by using two methods: (*i*) gas chromatography coupled to mass spectrometry (GC-MS; *SI Appendix*, Fig. S2*A*) and (*ii*) ^{3}H-L-Orn radiolabeling followed by high-performance liquid chromatography (HPLC) analysis and liquid scintillation counting (*SI Appendix*, Fig. S2*B*).

***B. burgdorferi* Sheds Muropeptides into Its Environment during Growth.** Because the *B. burgdorferi* genome appears to lack the requisite proteins (AmpG, AmpD, and LdcA) for muropeptide recycling (*SI Appendix*, Fig. S1*C*), we hypothesized that muropeptides produced during normal PG^{Bb} turnover are recycled via an unknown pathway or are released into the extracellular milieu. To determine whether PG recycling occurs, we pulse-labeled *B. burgdorferi* cells with L-Orn containing ^{3}H or ^{14}C isotopes, followed by cell outgrowth in radiolabel-free liquid culture medium. At various time points during outgrowth, we collected cells, purified PG^{Bb}, and analyzed these PG preparations by liquid scintillation counting. On average, the PG^{Bb} lost 40 ± 2% of radiolabeled L-Orn per generation (Fig. 1*B*), consistent with the lack of a muropeptide recycling pathway (34, 36). Moreover, we found that PG^{Bb} turnover during *B. burgdorferi* growth resulted in time-dependent muropeptide accumulation in the culture supernatant (Fig. 1*C* and *SI Appendix*, Fig. S3), similar to what is observed with mutant strains of other bacteria that lack the PG recycling permease AmpG required for cytoplasmic import of muropeptides (36–39). We showed this muropeptide release by exposing human NOD2 (hNOD2) reporter cells to *B. burgdorferi* culture supernatant samples. In these cells, binding of PG material containing Mur*N*Ac-L-Ala-D-Glu to the hNOD2 receptor drives downstream activation of NF-κB (42). Treatment with gefitinib, an inhibitor of the adaptor protein RIP2 downstream of NOD2 (43), prevented NF-κB activation (Fig. 1*C*). In addition, NF-κB signaling was not activated when we exposed human NOD1 reporter cells to *B. burgdorferi* culture supernatants (*SI Appendix*, Fig. S3). NOD1 specifically recognizes PG containing DAP in the third amino acid position of the stem peptide (44). Collectively, these results demonstrate that *B. burgdorferi* sheds muropeptides into its local environment, likely because it is unable to recycle them.

Patients with LA Develop an Adaptive Immune Response against *B. burgdorferi* PG. Animals, including humans, produce a humoral response that can discriminate different types of PG chemistry (45, 46). As the chemical composition of PG^{Bb} is unusual (Fig. 1*A* and *SI Appendix*, Table S1) (32), we postulated that it may contain epitopes that induce a specific immunoglobulin G (IgG) response capable of discriminating between PG^{Bb} and other bacterial PGs. To test this idea, we used purified PG from *B. burgdorferi* (Orn-type PG), *Escherichia coli* (DAP-type PG), *Bacillus subtilis* (amidated DAP-type PG), and *Staphylococcus aureus* (Lys-type PG) in an ELISA to probe for an anti-PG IgG response in 82 blinded synovial fluid samples from patients with different forms of arthritis. Some samples originated from patients with LA and included single and longitudinal samples. These samples were collected before treatment with oral antibiotics, after oral antibiotic treatment, or after oral antibiotic treatment and additional IV antibiotic therapy (*Methods*). Control synovial fluid samples from patients with rheumatoid arthritis, osteoarthritis, ankylosing spondylitis, or gouty arthropathy were randomly scattered among the coded samples. Another control synovial fluid sample was from a patient with a torn anterior cruciate ligament (ACL), which was the only nonblinded patient sample in our study.

We found that most LA synovial fluid samples contained significant levels of IgG antibodies against *B. burgdorferi* PG (anti-PG^{Bb}), whereas control samples from patients with other forms of arthritis or a torn ACL did not (Fig. 2 *A*, *Inset*). This IgG response was largely specific to PG^{Bb}, as LA samples displayed little to no IgG reactivity to PGs from other bacteria (Fig. 2*B*). In contrast, control samples did not exhibit a PG-specific IgG response (Fig. 2*C*). The levels of anti-PG^{Bb} IgG in preoral, postoral, and postoral/IV antibiotic LA patients did not significantly

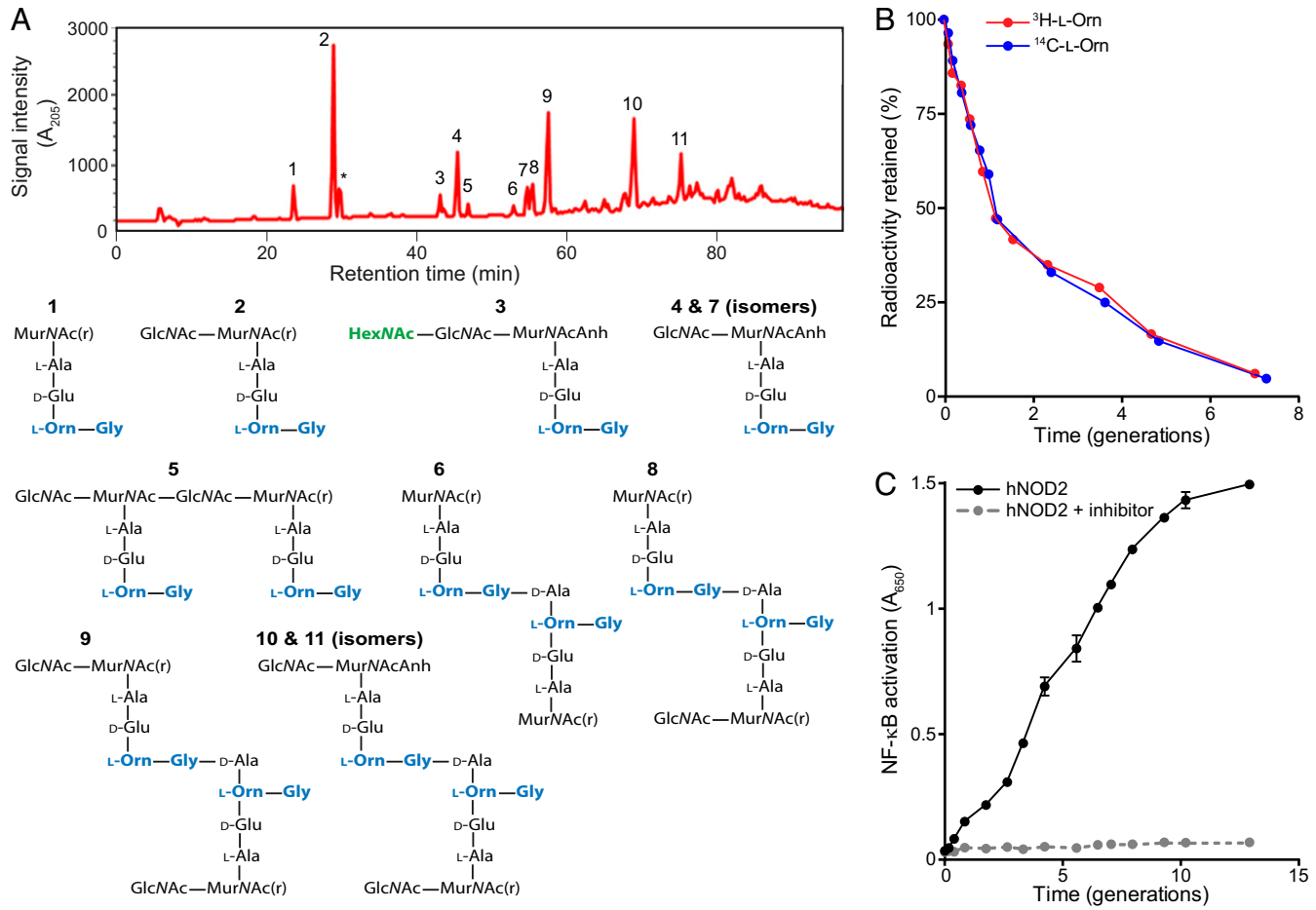

Fig. 1. *B. burgdorferi* sheds muropeptides into its extracellular environment. (*A*, *Top*) Chromatogram of cellosyl-digested and reduced PG^{Bb} isolated from *B. burgdorferi* B31. Numbers correspond to the identified chemical species shown below. The asterisk indicates an unidentified species (*SI Appendix*, Table S1). Analysis performed on three separate preparations produced highly similar chromatograms. (*A*, *Bottom*) Chemical composition of muropeptides in peaks shown in the chromatogram. Muropeptide identification was accomplished by MS. MurNAc(r) and Anh indicate *N*-acetylmuramitol and 1,6-anhydro group, respectively. (*B*) Plot showing PG turnover over multiple generations in *B. burgdorferi* grown in vitro. PG^{Bb} was pulse-radiolabeled by incubating cells in medium containing 7.5 μCi/mL of ^{3}H- or ^{14}C-L-Orn for 48 h. Cells were then washed to remove unincorporated isotope, and outgrowth was tracked in complete BSK II medium lacking radioactive L-Orn. At each time point, the same volume of batch culture was removed, bacterial density was determined, and PG^{Bb} was purified for quantification of its radioactivity per volume equivalent. The retained radioactivity was then plotted as a percentage of total radioactivity in the PG at time 0 (i.e., start of outgrowth). (*C*) Muropeptide accumulation in the culture medium. Cultures of *B. burgdorferi* (5×10^{7} cells per milliliter) were diluted to a starting density of 10^{4} cells per milliliter and monitored for muropeptide release during growth in complete BSK II medium (lacking phenol red) using an hNOD2 reporter cell line in the presence or absence of the RIP2 inhibitor gefitinib. NF-κB activity (absorbance at 650 nm) provides a measure of NOD2-specific muropeptide levels present in the culture medium samples collected at the indicated time points. Shown are the mean and SD of NF-κB activation for two biological replicates at each time point.

differ based on a Kruskal–Wallis test followed by a Dunn's post hoc pairwise test (*SI Appendix*, Fig. S4*A*). Several control samples contained anti-PG IgG levels above background (Fig. 2*A*), especially those from patients with rheumatoid arthritis (38%). However, such anti-PG responses, which have been previously reported in patients with rheumatoid arthritis (47, 48), were not specific for a particular type of PG tested (Fig. 2*A*).

From the original panel of synovial fluid samples, we had matching serum samples for 34 patients with LA (*Methods*), which we used as a subset for further analysis. We found that sera from LA patients contained significantly more anti-PG^{Bb} IgG than control sera from healthy people (Fig. 2*D*). Whereas the synovium represents a local environment, the synovial cavity communicates freely with systemic circulation, which likely explains why anti-PG^{Bb} IgG levels in paired serum and synovial fluid samples correlate (Fig. 2*E*). In all LA cases, the synovial fluid had a higher anti-PG^{Bb} IgG level than the corresponding serum sample from the same patient (Fig. 2*E*). Our data indicate that patients with LA produce specific antibodies against PG^{Bb} and that these responses are primarily localized to the joint, the site of inflammation.

***B. burgdorferi* PG Material Is Detected in Synovial Fluid Samples from Patients with LA after Antibiotic Treatment.** As patients with LA produce a specific anti-PG^{Bb} IgG response, we next sought to determine whether we could detect antigenic PG^{Bb} material in the synovial fluid of patients with LA. To this end, we generated a polyclonal anti-PG^{Bb} antiserum through immunization of New Zealand White rabbits with PG^{Bb}. The polyclonal antiserum was specific for PG^{Bb}, as it did not react with other common PG types in a competitive ELISA (*SI Appendix*, Fig. S5). By using this same competitive ELISA, we did not detect PG^{Bb} in control synovial fluid samples (Fig. 3*A*). We also failed to detect PG^{Bb} in the sera of patients with LA (Fig. 3*A*). However, 92% of the tested LA synovial fluid samples contained tens to hundreds of picograms of PG material per milliliter (Fig. 3*A*). The amount of PG detected strongly correlated with the anti-PG^{Bb} IgG level

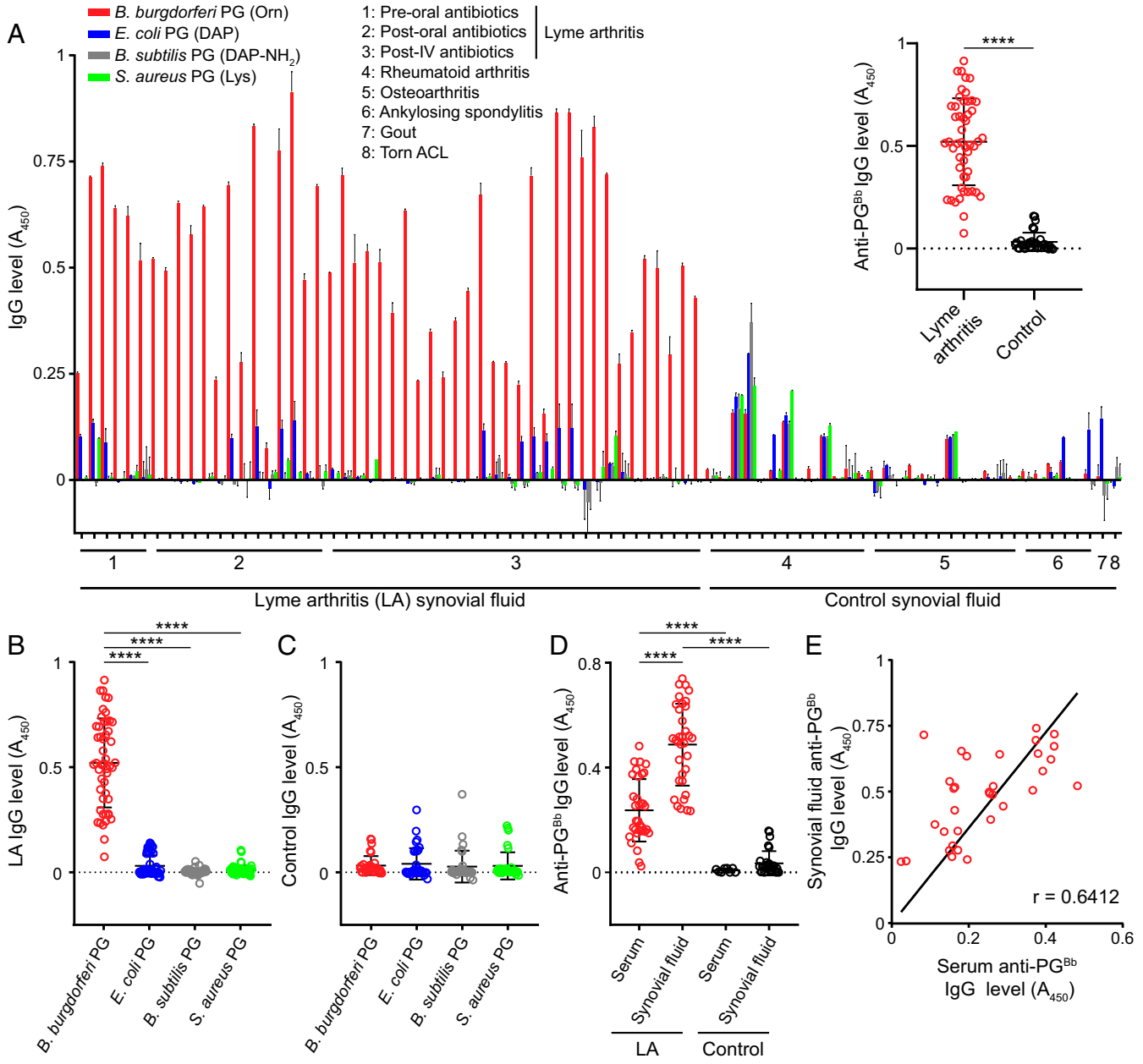

Fig. 2. Patients with LA develop an adaptive immune response specifically to PG^{Bb}. Purified PG from *B. burgdorferi* B31, *E. coli* K-12, *S. aureus* SA113, or *B. subtilis* 168 was immobilized, and synovial fluid from patients with different types of arthritis (groups 1–6 and 7) were blindly assayed for the presence of IgG by ELISA (****$P < 0.0001$, Kruskal–Wallis test followed by Dunn's post hoc pairwise test for *B* and Mann–Whitney *U* test for *A* and *D*). Horizontal black lines indicate means and SDs. (*A*) Levels of IgG against different PG types. After the results were obtained, the patient sample type was decoded and organized based on the arthritis type and treatment stage. Results for a control joint fluid sample obtained from a patient with a torn ACL (group 8) were also included. Values were background-subtracted based on the IgG level measured for each individual sample in the absence of PG ligand. (*Inset*) All anti-PG^{Bb} IgG values are shown as a bee-swarm plot for LA samples and controls (all non-LA samples). (*B*) Specificity of IgGs from LA synovial fluid samples for PGs from different bacteria. (*C*) Specificity of IgGs from control synovial fluid samples for different PG types. (*D*) Comparison of IgG responses to PG^{Bb} for serum and synovial fluid samples from patients with LA relative to those for serum from healthy humans and synovial fluid samples from control (non-LA) patients. (*E*) Correlation analysis of anti-PG^{Bb} IgG responses between the serum and synovial fluid of patients with LA. The linear fit and Pearson correlation coefficient (*r*) for the LA synovial fluid samples are also shown.

found in the same synovial fluid sample (Fig. 3*B*), indicating that the antigenic material detected by our rabbit polyclonal antiserum is likely PG^{Bb}. Our results show that PG^{Bb} is present in LA synovial fluid samples before and after oral and IV antibiotic treatment (*SI Appendix*, Fig. S4*B*).

PCR analysis showed that serum and synovial fluid samples were often positive for *B. burgdorferi* DNA before antibiotic treatment (*SI Appendix*, Fig. S4*C*). In contrast, all but one serum and synovial fluid sample were negative after oral antibiotic treatment and all samples were negative after IV antibiotic therapy (*SI Appendix*, Fig. S4*C*). Thus, our results suggest that PG^{Bb} material persists in LA patients long after *B. burgdorferi* eradication.

***B. burgdorferi* PG Elicits Proinflammatory Cytokine Responses in Human Peripheral Blood Mononuclear Cells.** LA is characterized by marked synovial hypertrophy and inflammation. As in other

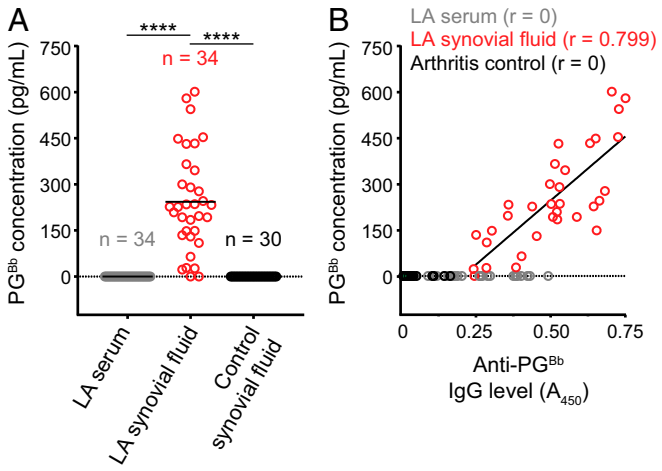

Fig. 3. Detection of PG^{Bb} in synovial fluid samples of patients with LA. (*A*) Competitive ELISA using rabbit antiserum raised against PG^{Bb} to quantify the concentration of PG (in picograms per milliliter) present in each sample. Horizontal black lines indicate means (****$P < 0.0001$, Kruskal–Wallis test followed by Dunn's post hoc pairwise test). (*B*) Plot showing the PG^{Bb} concentration of each sample as a function of its anti-PG^{Bb} IgG level. The linear fit and the Pearson correlation coefficient (r) for the LA synovial fluid samples are also shown.

forms of inflammatory arthritis, proinflammatory cytokines such as IL-1, TNFα, IL-6, and IL-8 are found in the synovial fluid of patients with LA (12, 49, 50). Consistent with these previous observations, we found that virtually all major proinflammatory markers were significantly up-regulated in the synovial fluid of patients with LA relative to their serum (*SI Appendix*, Fig. S6), ranging from 4- to 2,000-fold increases in TNFα, IL-1α, IL-1β, IL-6, IL-8, IL-17F, and INFγ production (Fig. 4*A*). Inflammation of this magnitude often coincided with a secondary response involving production of antiinflammatory cytokines, including IL-10, the level of which was also significantly increased in the synovial fluid of LA patients (*SI Appendix*, Fig. S6).

To determine if PG^{Bb} alone can elicit an inflammatory response, we stimulated human peripheral blood mononuclear cells (PBMCs) from healthy control subjects with polymeric (whole) or mutanolysin-digested PG^{Bb} for 18 or 72 h. The synthesis of virtually all analytes highly represented in synovial fluid samples (Fig. 4*A*) and previously implicated in LA (12, 50) was induced by polymeric and/or digested PG^{Bb} (Fig. 4*B* and *SI Appendix*, Fig. S7*A*). Note that, under these stimulatory conditions, PG^{Bb} behaves similarly to other PG types (*SI Appendix*, Fig. S7). However, stimulation with PG^{Bb} resulted in only a two- to threefold increase in the level of antiinflammatory cytokine IL-10 after 72 h relative to the 10-fold increase seen with other PG types (Fig. 4*B* vs. *SI Appendix*, Fig. S7). These findings suggest that PG^{Bb} may have the ability to cause inflammation without eliciting a compensatory antiinflammatory response of the magnitude normally seen with infectious agents and associated immunogens (51).

Systemic Administration of *B. burgdorferi* PG Triggers Acute Arthritis in Mice. Systemic injection of PG isolated from Gram-positive bacteria is known to induce arthritis in mice and rats (23–26). To test the arthritogenic potential of the chemically unusual PG^{Bb}, we injected a sonicated preparation of PG^{Bb} into the tail veins of 12 BALB/c mice. In parallel, a control group of 12 mice received the diluent (PBS). All 24 mice were evaluated clinically and scored daily for evidence of swelling and erythema in their paws and tibiotarsal joints. Half of the mice from each group were

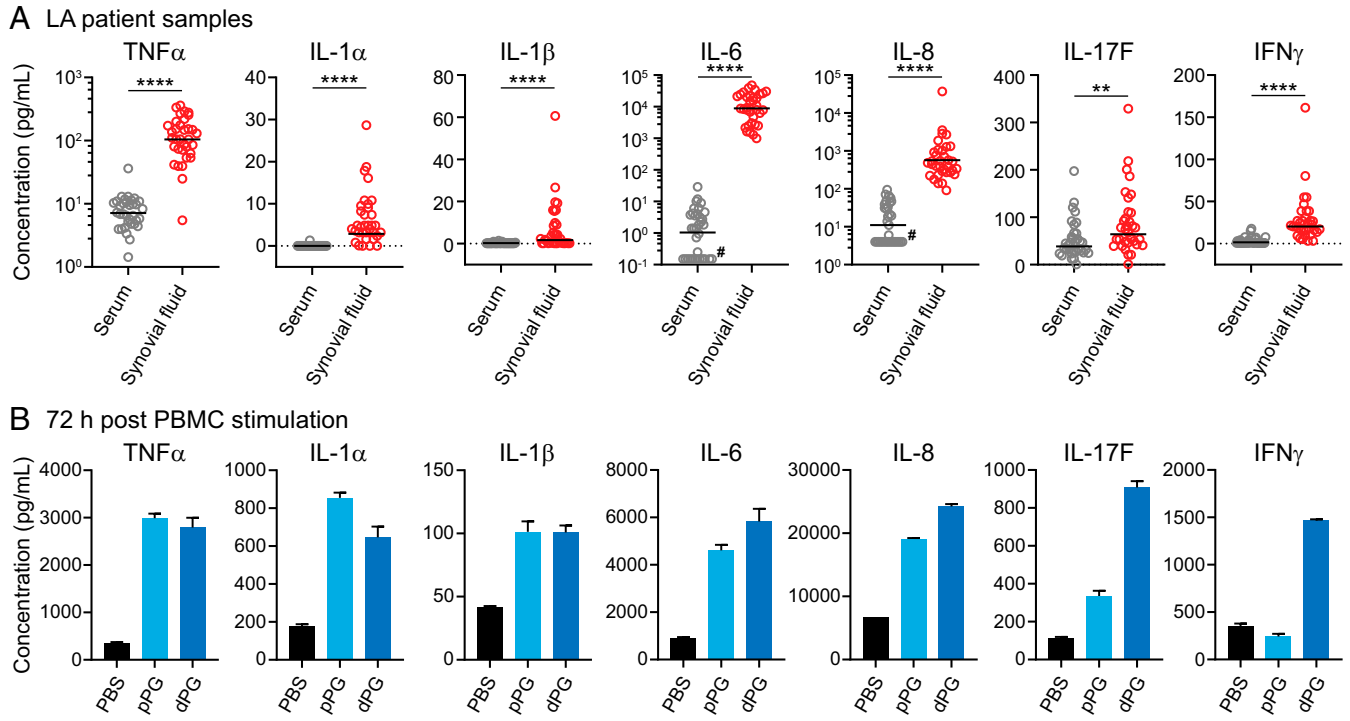

Fig. 4. Cytokine profile in serum and synovial fluid samples from patients with LA or after in vitro stimulation of human PBMCs with PG^{Bb}. (*A*) Bee-swarm plots showing levels of indicated cytokines in LA patient samples. Horizontal black lines indicate geometric means (****$P < 0.0001$ and **$0.001 < P < 0.01$, Mann-Whitney U test). Pound signs indicate samples that yielded no signal but were included for completeness, as zero values cannot be displayed on log-scale axes. (*B*) Cytokine levels produced by control human PBMCs stimulated by PBS or 100 μg/mL polymeric PG (pPG) or mutanolysin-digested PG (dPG) for 72 h. The 18-h results are shown in *SI Appendix*, Fig. S7*A*. All stimulatory studies were performed on pooled, mixed donor samples assayed in duplicate (mean ± SD).

randomly selected and euthanized on day 2 or 4 postinjection. Both hind limbs from each euthanized animal were immersion-fixed, decalcified, and stained with hematoxylin-eosin for blinded histopathological evaluation (52).

We found that PG^{Bb} alone was sufficient to induce acute arthritis, as evidenced by ankle swelling by 24–96 h postinjection (Fig. 5 *A*–*C*). In contrast, the control mice injected with PBS alone, as well as additional unmanipulated mice housed under similar conditions, showed no visual evidence of swelling (Fig. 5 *A*–*C*). Histopathologic analysis of the hind limbs of mice injected with PG^{Bb} confirmed the presence of inflammatory infiltrates in the peritendinous adventitia (Fig. 5 *E*, single pound symbols) and edema in the synovial space (Fig. 5 *E*, double pound symbols) at 48-h and 96-h time points (Fig. 5 *D* and *E*). Such infiltrates were absent in control mice injected with PBS (Fig. 5 *D* and *E*). Our data indicate that systemic exposure to PG^{Bb} is sufficient to trigger an acute tenosynovitis, consistent with what is observed in the established mouse model of LA (53).

Discussion

Our study provides supporting evidence of an important role for PG^{Bb} in the pathogenesis of LA. Clinical manifestations of Lyme disease are largely driven by the host immune response rather than toxin-mediated damage (6). PG is recognized by several types of pattern recognition receptors including Toll-like receptors (TLRs), PG recognition proteins (PGRPs), and cytoplasmic NOD proteins (22, 54). Although their downstream effectors may vary (55), the result is often a strong proinflammatory response (56). Similar inflammatory responses are apparent in the synovial fluid of patients with LA based on cytokine profiling (Fig. 4 and *SI Appendix*, Fig. S6). For instance, TNFα was, on average, up-regulated 16-fold in synovial fluid samples from patients with LA and induced in human PBMCs exposed to PG^{Bb} in vitro (Fig. 4 and *SI Appendix*, Fig. S7*A*). This is noteworthy, as TNFα is a key effector protein in chronic inflammatory arthritides, and biologic agents targeting TNFα have been used successfully in cases of postinfectious LA (5).

Although autoimmunity has been implicated in the pathogenesis of LA (9–13, 57), genetic and transcriptomic evidence suggests that variability in innate immune responses during and after *B. burgdorferi* infection is also an important disease determinant. Notably, transcripts encoding PG-cleaving protein lysozyme and PG-sensing protein NOD2 are elevated in synovial tissues of postinfectious LA patients months to several years after antibiotic therapy (58, 59). Therefore, immune responses to PG^{Bb} and autoantigens may contribute to pathology, even after the infection itself has been cleared. The role of PG^{Bb} and autoantigens may be independent or PG^{Bb} may act as an adjuvant, exacerbating immunoreactivity to autoantigens in the synovium. Differences in PG^{Bb}-specific immune responses among patients with LA may contribute to variability in disease severity.

How can PG^{Bb} material remain in the synovial environment for an extended period (weeks to months) after appropriate antibiotic treatment (Fig. 3)? There are several possibilities.

First, PG material may be left behind after bacterial killing. *B. burgdorferi* cells that disseminate to the joint may shed muropeptides as they undergo replication. These muropeptides may then diffuse into the synovial cavity over time. Alternatively (or in addition), PG exposure may occur in the absence of spirochete replication; PG material may simply be released following bacterial lysis (through natural death or killing by the immune system or antibiotic treatment). Both possibilities would

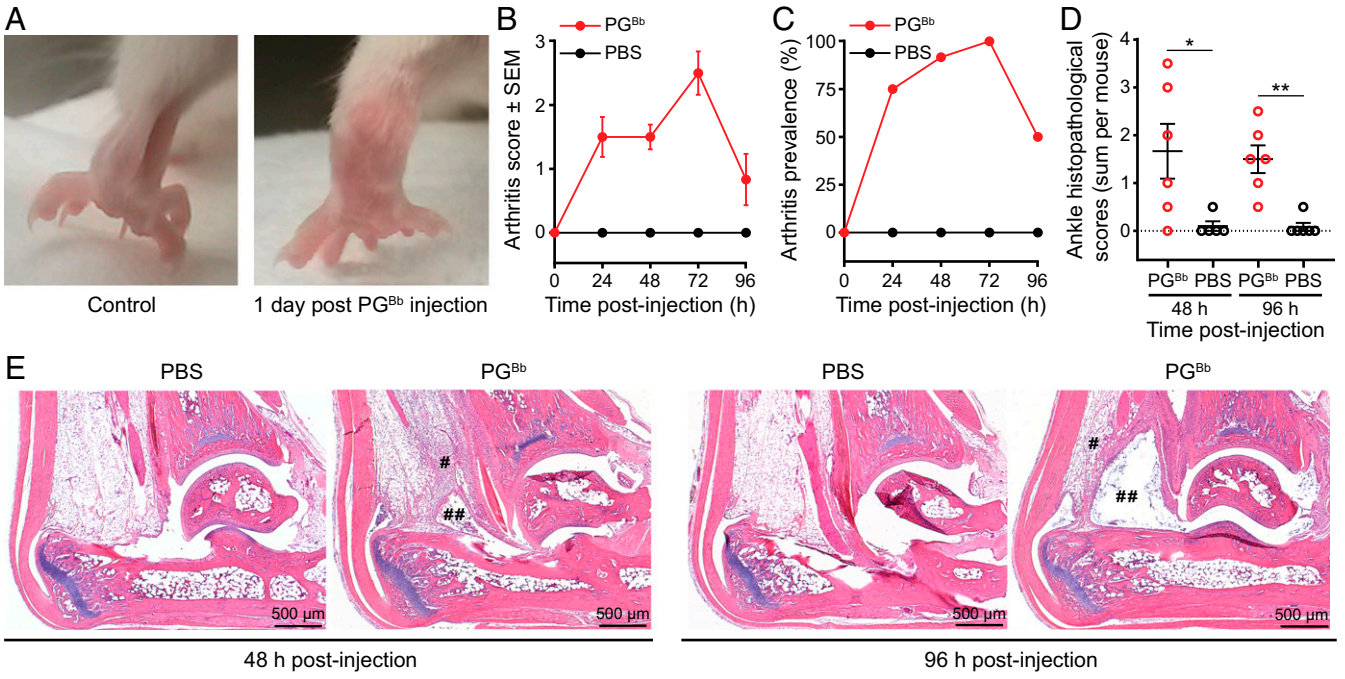

Fig. 5. Systemic administration of PG^{Bb} induces acute arthritis in mice. (*A*) A BALB/c mouse 24 h after IV injection of 200 μg PG^{Bb} exhibits bilateral ankle edema not present in an uninjected control mouse. (*B*) Average composite arthritis score (i.e., average sum of individual scores for left and right hind limbs) within each mouse group 24, 48, 72, and 96 h after IV administration of PG^{Bb} or PBS. Error bars indicate SEMs; $n = 12$ mice per group at 24 and 48 h postinjection and $n = 6$ mice per group at all subsequent time points. (*C*) Arthritis prevalence as a function of time after injection with PG^{Bb} or PBS. Only mice with a composite arthritis score ≥1 were considered as having arthritis. (*D*) Sum of left and right ankle histopathological scores for individual mice at 48 or 96 h after IV injection of PG^{Bb} or PBS. Horizontal black lines indicate means and SEM (**$P < 0.01$ and *$0.01 < P < 0.05$, respectively, Mann–Whitney *U* test). (*E*) Representative light micrographs of hematoxylin-eosin–stained sections of mouse ankles collected 48 or 96 h after IV administration of PG^{Bb} show peritendon inflammation (single pound symbols) and synovial space edema (double pound symbols). PBS-injected control mice lack both histopathological features when examined at the same time points.

be consistent with the hypothesis that retained bacterial antigens are a source of inflammatory stimuli in LA (14). In rats, bacterial cell-wall fragments are detected weeks to months after their systemic administration (60, 61), supporting the notion that PG material can persist for an extended period in animals.

Second, tissue-resident synovial macrophages may act as an antigen sink (62). Although our synovial samples were free of cells (*Methods*), they contained extracellular vesicles, likely derived from immune and stromal cells (63). Vesicles from antigen-presenting cells containing PG^{Bb} material may be released into the surrounding environment. Interestingly, antigen-presenting cells containing PG from gut bacteria have been proposed to contribute to inflammation in patients with rheumatoid arthritis (64, 65).

Third, PG-containing immune complexes may accumulate in the synovial fluid. We show that patients with LA develop a specific anti-PG^{Bb} antibody response that is higher in the synovial fluid than in the serum (Fig. 2). This, together with the presence of PG^{Bb} in the synovial fluid (Fig. 3), may result in accumulation of PG^{Bb} immune complexes in the inflamed joints. Previous work on *Bacillus anthracis* PG has established that PG can form immune complexes with anti-PG antibodies, which can activate human platelets and promote vascular damage (66). Inflammation and damage in and around the microvasculature is a hallmark of the synovial lesions seen in postinfectious LA (67, 68), and immune complexes are known to localize to joints in patients with LA (69). Future studies will be required to discriminate between these three nonexclusive possibilities.

The finding that *B. burgdorferi* releases PG^{Bb} fragments during growth (Fig. 1*C*) suggests that PG^{Bb} may play a broad role in the multifaceted pathogenesis of Lyme disease beyond LA. Released muropeptides have previously been implicated in diseases caused by other bacteria. For example, *Neisseria gonorrhoeae* recycles most of its PG breakdown products (39, 70), as Gram-negative bacteria generally do. However, the small amount of PG monomers that *N. gonorrhoeae* releases (39, 71) is thought to induce inflammatory cytokine production and cause ciliated cell death in human fallopian tubes (72). In contrast to *N. gonorrhoeae*, *B. burgdorferi* lacks a PG recycling pathway (Fig. 1*B* and *SI Appendix*, Fig. S1*C*), suggesting that significant quantities of muropeptides may be released into the environment during *B. burgdorferi* proliferation, presumably through the outer-membrane porins. We confirmed that hNOD2-binding muropeptides are shed into the culture supernatant during *B. burgdorferi* growth (Fig. 1*C*). Given PG^{Bb} immunogenicity (Figs. 2, 4, and 5 and *SI Appendix*, Fig. S7) (32), muropeptide shedding during active *B. burgdorferi* infection may, together with surface-exposed lipoproteins (73–75) and glycolipids (76, 77), contribute to early inflammatory manifestations, such as skin lesions, carditis, and meningitis.

After antibiotic treatment of the infection, therapy for postinfectious LA is currently directed at dampening immune responses with disease-modifying antirheumatic drugs, primarily hydroxychloroquine or methotrexate (5). The persistence of immunogenic PG^{Bb} material in inflamed joints provides a stronger rationale for targeting innate immune responses with medications, such as TNF or NF-κB inhibitors, for the treatment of such patients. A potential role for bacterial PG in triggering inflammation in rheumatoid arthritis patients has been considered for several decades (61, 62, 64, 65). Our work supports further consideration of this idea.

Methods

Bacterial Strains, Cell Lines, and Growth Conditions. A clone of the *B. burgdorferi* type strain B31 (MI) (16) was used in all experiments involving this bacterium. Other bacteria used in this study include *S. aureus* SA113, *B. subtilis* 168, and *E. coli* K-12 MG1655. Unless otherwise noted, *B. burgdorferi* was cultured at 34 °C in complete BSK II medium containing 6% rabbit serum (78). All other bacteria were grown at 37 °C in LB medium. HEK 293-derived human NOD1 and NOD2 reporter cell lines (InvivoGen) were cultured at 37 °C under 5% CO_2 in RPMI medium containing 10% (vol/vol) FBS and blasticidin S (30 μg/mL), Zeocin (100 μg/mL), and Normocin (100 μg/mL). Fresh PBMCs from healthy human subjects were obtained from mixed donor samples (Zen-Bio) and used in assays in the recommended PBMC culture medium (Zen-Bio).

PG Purification. PG^{Bb} was purified as described previously (79), which is an adaptation of the Glauner protocol (80). For immunological and mouse studies, a few modifications were made to increase yield and ensure purity. PG^{Bb} was purified from 2–3 L of *B. burgdorferi* culture. Before protease treatment with 300 μg/mL α-chymotrypsin (Sigma-Aldrich), insoluble PG^{Bb} was treated with 50 U of DNase (Zymogen) and 10 U of RNase A (Promega) for 2 h, followed by a 2-h treatment with 10 μg/mL amylase (Sigma-Aldrich). After protease digestion, PG^{Bb} sacculi were harvested and washed three times with 10 mL endotoxin-free water, once with 10 mL 0.5 M EDTA, and three more times with water. A similar procedure was performed to purify PG from *E. coli*. For PG preparations from Gram-positive bacteria, the cell walls were broken using a kit (Precellys Microorganism Lysing Kit) that includes 7-mL tubes containing glass beads before sodium dodecyl sulfate (SDS) solubilization and enzymatic treatment. The Precellys Evolution homogenizer was set to 10 cycles of 30 s at 8,500 rpm with a 60-s rest period between each cycle. Afterward, samples were treated with 48% hydrofluoric acid for 48 h at 4 °C to hydrolyze PG-bound teichoic acids as previously described (81). Post hydrolysis, PG sacculi were harvested and washed as described here earlier.

The concentration of all purified PG preparations was determined by dry weight and confirmed by SLP assay as previously described (82).

PG Structural and Chemical Analysis. Purified PG^{Bb} (~100 μg) was digested with cellosyl (25 μg/mL) for 14–16 h at 37 °C, and the resulting muropeptides were analyzed by LC-MS as reported previously (83).

For the chemical analysis, purified PG^{Bb} (0.7 mg) was hydrolyzed (200 μL 4 N HCl, 100 °C, 16 h) in a sealed ampoule. The hydrolysate was evaporated to dryness in a gentle stream of air at 60 °C. The residue was dissolved in 200 μL water and dried down again to remove residual HCl. The amino acids of the hydrolysate were transformed into *N*-pentafluoropropionyl amino acid isopropylesters according to protocol 11 described in a previous review (84). These amino acid derivatives were analyzed by GC (GC-14A; Shimadzu) with a CP-ChiraSil-L-Val column (Agilent Technologies, CP495) following protocol 11 and by GC-MS using a 320 Single Quad instrument (Varian) equipped with a VF-5ms column (CP8944; Agilent Technologies) using protocol 10 (84).

To verify the incorporation of L-Orn into the PG^{Bb} (*SI Appendix*, Fig. S2*B*), *B. burgdorferi* was cultured in 500 mL complete BSK II medium to a density of 10^6 cells per milliliter. Cells were harvested by centrifugation (3,500 × *g* for 20 min) and resuspended in 50 mL of prewarmed, modified medium (25% BSK II in PBS plus 1.2% rabbit serum) (85) containing 7.5 μCi/mL of ^{3}H L-Orn (Perkin-Elmer). After 48 h of incubation, unincorporated radiolabeled L-Orn was removed by centrifugation (3,500 × *g* for 20 min) and three washes with 40 mL of PBS. After each wash, cells were harvested by centrifugation at 3,500 × *g* for 10 min. After the washes, the cells were gently resuspended in 5 mL of PBS and PG was purified as described earlier.

PG Turnover Studies. To track the turnover of PG^{Bb} over time (Fig. 1*B*), we used two different protocols. In the first one, 500 mL culture of *B. burgdorferi* at a cell density of 10^6 cells per milliliter was pulse-labeled with 7.5 μCi/mL of ^{14}C L-Orn as described earlier. After three washes and centrifugation, cells were gently resuspended to a final concentration of 5×10^4 cells per milliliter in 250 mL prewarmed BSK II complete medium [which includes rabbit serum that contains Orn (86)]. Retention of radiolabel into the PG^{Bb} was tracked by removing a 25-mL culture volume at various time points, harvesting the cells by centrifugation (3,500 × *g* for 20 min), washing cells once with 25 mL of PBS, and harvesting cells at 3,500 × *g* for 10 min. Pelleted cells were resuspended, and cells were solubilized in a boiling solution of 4% SDS for 30 min. SDS-insoluble PG^{Bb} was pelleted at 145,000 × *g* for ~30 min and analyzed by liquid scintillation. In the second protocol, a 250-mL culture of *B. burgdorferi* at 10^6 cells per milliliter was centrifuged (4,000 × *g* for 20 min) and cells were resuspended in 50 mL of prewarmed, modified medium (as described earlier) containing 7.5 μCi/mL of ^{3}H L-Orn. After 48 h of incubation, unincorporated radiolabeled L-Orn was removed by centrifugation (4,000 × *g* for 20 min) and three washes with 40 mL of PBS. After each wash, cells were harvested by centrifugation at 3,000 × *g* for 10 min. After washes, cells were resuspended in 125 mL of BSK II complete medium at a density of 5×10^4 cells per milliliter. The remaining steps were the same as the first protocol except that 10 mL of culture was removed at each time point and cells were harvested at 4,000 × *g* for 20 min. Both protocols gave highly similar results (Fig. 1*B*).

NOD Activation Assay. Time-course experiments to monitor the release of muropeptides were performed to ensure that potential stress during the radiolabeling procedure (as detailed earlier) or washes did not significantly alter our findings. In these experiments, 10 mL of culture was removed from a 250-mL batch culture, cells were enumerated, and 8 mL of culture was filtered by using a 0.1-μm filter under a vacuum. From the filtered flow-through, 5 mL was processed through a YM-3 Amicon filter to selectively exclude biomolecules greater than 3,000 Da. Column flow-through (4 mL) was lyophilized and resuspended in 1 mL of endotoxin-free Dulbecco's PBS (DPBS), resulting in a 4× solution of the culture supernatant. Sterile BSK II complete medium (without phenol red) was processed similarly to serve as control medium to which each signal was background-subtracted.

HEK-Blue hNOD1 and hNOD2 cells were cultured to 60–70% confluence, washed with PBS, enumerated, and resuspended in QUANTI-Blue detection medium (InvivoGen) at a final concentration of 2.5×10^5 cells per milliliter. HEK-Blue hNOD1 or hNOD2 cells (180 μL per well) were incubated in 96-well plate in triplicate with 20 μL of a three-time dilution (in DPBS) of the 4× culture-supernatant solution. Cells were incubated at 37 °C in 5% CO_2 for 18 h. Colorimetric quantification of NF-κB activity through NOD1 or NOD2 activation was measured at 650 nm. Gefitinib (Sigma), an inhibitor that interferes with adaptor protein RIP2 signaling (43), was used at a final concentration of 20 μM.

Human Subject Samples. All work with human samples was approved by the human investigations committee at Massachusetts General Hospital granted to A. Steere. Patients with Lyme disease satisfied the criteria put forth by the Centers for Disease Control and Prevention (87). Patients with LA were treated with 1–2 mo of oral antibiotic therapy (usually doxycycline), followed by an additional 1 mo of IV antibiotic therapy (ceftriaxone) if needed, as described by the Infectious Diseases Society of America (88). Control synovial fluid samples were acquired from patients with rheumatoid arthritis, psoriatic arthritis, and osteoarthritis who met the criteria associated with each disease (89–91).

Serum and synovial fluid samples were collected and then centrifuged at 300 × *g* for 10 min, followed by another centrifugation at 3,000 × *g* for another 10 min to remove cells and cell debris as previously described (92). All samples were stored at −80 °C and did not undergo more than two freeze–thaw cycles.

PCR Analysis. Serum and synovial fluid samples were screened by PCR for amplification of the *B. burgdorferi flaB* gene by using the fla-3 (5′-GGGTCTCAAGCGTCTTGG-3′) and fla-4 (5′-GAACCGGTGCAGCCTGAG-3′) oligonucleotides and Phusion Polymerase (New England Biolabs). The cycling conditions were as follows: 1 cycle at 98 °C for 30 s and 45 cycles of 98 °C for 12 s, 58 °C for 20 s, and 70 °C for 15 s, followed by a final extension at 70 °C for 5 min. All reactions were subjected to DNA agarose electrophoresis and visualized by ethidium bromide staining. Visible products were apparent for serum samples 9, 13, 17, 20, and 33 and for synovial fluid samples 9, 13, 17, and 20 (*SI Appendix*, Fig. S4*C*).

ELISA. To quantify the level of anti-PG IgG in patient samples, purified PG sacculi (100 μg/mL) in PBS with 0.01% SDS were immobilized on poly-lysine–coated microtiter plates overnight at 4 °C. Unbound material was removed through three washes with PBS-T (PBS plus 0.05% Tween 20). The wells were then "blocked" for 2 h at 37 °C using SEA-BLOCK (Thermo Fisher Scientific). Serum and synovial fluid samples were diluted 1:25 in PBS and incubated with substrates (or diluent control) for 2 h at room temperature with gentle rocking. Unbound material was washed with PBS-T. After washing, plates were incubated with anti-human IgG-HRP (1:25,000; Sigma-Aldrich), and bound IgG was detected by using 1-step Turbo TMB substrate (Thermo Fisher Scientific). Reported IgG response was determined by measuring absorbance at 450 nm, following background subtraction for each patient sample signal attained in the absence of PG ligand.

Detection of PG^{Bb} in patient samples was performed by using a competitive ELISA and rabbit anti-PG^{Bb} polyclonal antibodies produced as a fee-for-service by Cocalico Biologicals (Thermo Fisher Scientific). Briefly, purified PG^{Bb} (0.5 mg/mL) was used to immunize two New Zealand White rabbits according to protocols approved by the animal care and use committee of Cocalico Biologicals. After one dose, two boosters of 0.5 mg/mL were administered 1 wk apart. Serum from blood samples collected on days 53 and 54 was assayed for PG^{Bb} specificity by competitive ELISA. Competitive ELISA involved coating plates with 100 μg/mL of PG^{Bb} as described earlier. Rabbit serum containing anti-PG^{Bb} IgG was diluted 1:350 in PBS and preincubated for 2 h with titrating amounts (10 ng/mL to 10 pg/mL) of different bacterial PG preparations with gentle mixing at room temperature before 1 h incubation with PG^{Bb}-coated plates. All patient samples were diluted 1:5 in PBS and otherwise treated exactly as the PG^{Bb} standards of known concentration. Rabbit anti-IgG-HRP (Bio-Rad) diluted 1:3,000 was used to detect anti-PG^{Bb}. Standard curves were created by using 1/absorbance values (at 450 nm) produced with known concentrations of each PG preparation. Data were fitted by a third-order polynomial equation. Standard curve experiments were performed on the same day as the serum and synovial fluid analyses and used to back-calculate the amount of PG^{Bb} in each patient sample.

PBMC Stimulation and Cytokine Analysis. Muropeptides were generated by digesting 1 mL of purified PG (120 μg/mL) with *Streptomyces globisporus* mutanolysin (1,000 U/mL; Sigma-Aldrich) for 4 h at 37 °C in buffer (50 mM MES, 1 mM $MgCl_2$, pH 6), followed by another incubation of mutanolysin (~500 U) overnight at 37 °C. Undigested material was harvested by centrifugation at 150,000 × *g* for 30 min at 12 °C. The soluble muropeptides were lyophilized, and their amount was determined by weight.

Upon arrival, fresh PBMCs (Zen-Bio) were seeded in 12-well plates at 10^6 cells per milliliter and allowed to rest at 37 °C under 5% CO_2 atmosphere for 24 h before further manipulation. After stimulation with 100 μg/mL of digested or polymeric PG, cells were harvested by centrifugation at 600 × *g* for 8 min and supernatants were collected and stored at −80 °C for further analysis. All cytokines were assayed using Luminex bead arrays (Agilent) following the manufacturer's recommendations. All supernatants were diluted 1:5 in PBS and analyzed in duplicate.

Serum and synovial fluid samples from patients with LA, diluted 1:3 in PBS, were similarly analyzed in duplicate and run on the same day as the PBMC supernatants. The concentration of cytokines (in picograms per milliliter) from patient samples were $\log_2$-transformed to create the heat map (*SI Appendix*, Fig. S6).

PG Injection in Mice and Histopathology. Purified PG^{Bb} was lyophilized, weighed, and resuspended to a final concentration of 2 μg/μL in DPBS. To achieve even dispersal PG^{Bb} in DPBS, the suspension was subjected to four rounds of sonication (15 s each) on ice using a Branson Digital Sonifier set to 45% amplitude. Fragmented PG^{Bb} (100 μL, i.e., 200 μg PG^{Bb}) was administered IV to each of 12 female BALB/c mice (5–6 wk old) by tail vein injection. In parallel, 12 BALB/c mice (age- and sex-matched) were injected IV with 100 μL DPBS. All mice were then examined daily for foot and ankle swelling and assigned a clinical arthritis score as previously described (29). Briefly, arthritis scores were computed by summing the individual scores for both hind paws, each graded as follows: 0, normal paw, no redness or swelling; 1, some swelling of ankle; 2, moderate swelling and redness of ankle; 3, moderate swelling and redness of ankle and some swelling of foot pad and/or digits; and 4, pronounced swelling and redness of the whole paw. Each group of mice was also evaluated for the prevalence of arthritis (defined as the percentage of mice with an arthritis score of at least 1). Half of the mice in each group ($n = 6$) were euthanized by CO_2 asphyxiation on days 2 and 4 postinjection, and both hind limbs from each animal were immediately fixed in 10% formalin and subsequently decalcified, embedded in paraffin, sectioned, and stained with hematoxylin-eosin by routine methods. For each mouse, one stained section per hind limb midlevel (to include the stifle and tibiotarsal joints) was analyzed. Sections were analyzed, and stifle and tibiotarsal inflammation was scored blindly by a veterinarian (C.J.B.) formally trained in pathology with years of experience in scoring mice for inflammation using previously published criteria (93). All procedures involving mice were approved by the Yale University Institutional Animal Care and Use Committee.

ACKNOWLEDGMENTS. We thank Alexia Belperron, Jialing Mao, and Nicole D'Angelo for assistance with the mouse experiments; Roman Dziarski for advice in planning the PG injection studies; and Dr. Patricia Rosa and the laboratories of C.J.-W. and B.L.J. for valuable discussions and critical reading of the manuscript. This study was supported in part by Wellcome Trust grant 101824/Z/13/Z (to W.V.) and National Institutes of Health grants AI101175 and AI144365. C.J.-W. is an investigator of the Howard Hughes Medical Institute.

1. P. S. Mead, Epidemiology of Lyme disease. *Infect. Dis. Clin. North Am.* **29**, 187–210 (2015).
2. G. Stanek, F. Strle, Lyme borreliosis-from tick bite to diagnosis and treatment. *FEMS Microbiol. Rev.* **42**, 233–258 (2018).
3. U. Koedel, V. Fingerle, H. W. Pfister, Lyme neuroborreliosis-epidemiology, diagnosis and management. *Nat. Rev. Neurol.* **11**, 446–456 (2015).
4. M. L. Robinson, T. Kobayashi, Y. Higgins, H. Calkins, M. T. Melia, Lyme carditis. *Infect. Dis. Clin. North Am.* **29**, 255–268 (2015).

5. S. L. Arvikar, A. C. Steere, Diagnosis and treatment of Lyme arthritis. *Infect. Dis. Clin. North Am.* **29**, 269–280 (2015).
6. L. K. Bockenstedt, G. P. Wormser, Review: Unraveling Lyme disease. *Arthritis Rheumatol.* **66**, 2313–2323 (2014).
7. D. Carlson *et al*., Lack of Borrelia burgdorferi DNA in synovial samples from patients with antibiotic treatment-resistant Lyme arthritis. *Arthritis Rheum.* **42**, 2705–2709 (1999).
8. X. Li *et al*., Burden and viability of Borrelia burgdorferi in skin and joints of patients with erythema migrans or Lyme arthritis. *Arthritis Rheum.* **63**, 2238–2247 (2011).
9. J. T. Crowley *et al*., A highly expressed human protein, apolipoprotein B-100, serves as an autoantigen in a subgroup of patients with Lyme disease. *J. Infect. Dis.* **212**, 1841–1850 (2015).
10. J. T. Crowley *et al*., Matrix metalloproteinase-10 is a target of T and B cell responses that correlate with synovial pathology in patients with antibiotic-refractory Lyme arthritis. *J. Autoimmun.* **69**, 24–37 (2016).
11. A. Pianta *et al*., Annexin A2 is a target of autoimmune T and B cell responses associated with synovial fibroblast proliferation in patients with antibiotic-refractory Lyme arthritis. *Clin. Immunol.* **160**, 336–341 (2015).
12. K. Strle *et al*., T-helper 17 cell cytokine responses in Lyme disease correlate with Borrelia burgdorferi antibodies during early infection and with autoantibodies late in the illness in patients with antibiotic-refractory Lyme arthritis. *Clin. Infect. Dis.* **64**, 930–938 (2017).
13. E. E. Drouin *et al*., A novel human autoantigen, endothelial cell growth factor, is a target of T and B cell responses in patients with Lyme disease. *Arthritis Rheum.* **65**, 186–196 (2013).
14. L. K. Bockenstedt, D. G. Gonzalez, A. M. Haberman, A. A. Belperron, Spirochete antigens persist near cartilage after murine Lyme borreliosis therapy. *J. Clin. Invest.* **122**, 2652–2660 (2012).
15. K. Takayama, R. J. Rothenberg, A. G. Barbour, Absence of lipopolysaccharide in the Lyme disease spirochete, Borrelia burgdorferi. *Infect. Immun.* **55**, 2311–2313 (1987).
16. C. M. Fraser *et al*., Genomic sequence of a Lyme disease spirochaete, Borrelia burgdorferi. *Nature* **390**, 580–586 (1997).
17. M. Hirschfeld *et al*., Cutting edge: Inflammatory signaling by Borrelia burgdorferi lipoproteins is mediated by toll-like receptor 2. *J. Immunol.* **163**, 2382–2386 (1999).
18. J. C. Salazar *et al*., Lipoprotein-dependent and -independent immune responses to spirochetal infection. *Clin. Diagn. Lab. Immunol.* **12**, 949–958 (2005).
19. M. R. Kenedy, T. R. Lenhart, D. R. Akins, The role of Borrelia burgdorferi outer surface proteins. *FEMS Immunol. Med. Microbiol.* **66**, 1–19 (2012).
20. W. Vollmer, D. Blanot, M. A. de Pedro, Peptidoglycan structure and architecture. *FEMS Microbiol. Rev.* **32**, 149–167 (2008).
21. A. Typas, M. Banzhaf, C. A. Gross, W. Vollmer, From the regulation of peptidoglycan synthesis to bacterial growth and morphology. *Nat. Rev. Microbiol.* **10**, 123–136 (2011).
22. A. J. Wolf, D. M. Underhill, Peptidoglycan recognition by the innate immune system. *Nat. Rev. Immunol.* **18**, 243–254 (2018).
23. S. A. Stimpson *et al*., Effect of acetylation on arthropathic activity of group A streptococcal peptidoglycan-polysaccharide fragments. *Infect. Immun.* **55**, 16–23 (1987).
24. A. Fox *et al*., Arthropathic properties related to the molecular weight of peptidoglycan-polysaccharide polymers of streptococcal cell walls. *Infect. Immun.* **35**, 1003–1010 (1982).
25. T. Koga *et al*., Acute joint inflammation in mice after systemic injection of the cell wall, its peptidoglycan, and chemically defined peptidoglycan subunits from various bacteria. *Infect. Immun.* **50**, 27–34 (1985).
26. T. Onta *et al*., Induction of acute arthritis in mice by peptidoglycan derived from Gram-positive bacteria and its possible role in cytokine production. *Microbiol. Immunol.* **37**, 573–582 (1993).
27. Z. Q. Liu, G. M. Deng, S. Foster, A. Tarkowski, Staphylococcal peptidoglycans induce arthritis. *Arthritis Res.* **3**, 375–380 (2001).
28. X. Li *et al*., CD14 mediates the innate immune responses to arthritopathogenic peptidoglycan-polysaccharide complexes of Gram-positive bacterial cell walls. *Arthritis Res. Ther.* **6**, R273–R281 (2004).
29. S. Saha *et al*., PGLYRP-2 and Nod2 are both required for peptidoglycan-induced arthritis and local inflammation. *Cell Host Microbe* **5**, 137–150 (2009).
30. M. Oosting *et al*., Recognition of Borrelia burgdorferi by NOD2 is central for the induction of an inflammatory reaction. *J. Infect. Dis.* **201**, 1849–1858 (2010).
31. T. Petnicki-Ocwieja *et al*., Nod2 suppresses Borrelia burgdorferi mediated murine Lyme arthritis and carditis through the induction of tolerance. *PLoS One* **6**, e17414 (2011).
32. G. Beck, J. L. Benach, G. S. Habicht, Isolation, preliminary chemical characterization, and biological activity of Borrelia burgdorferi peptidoglycan. *Biochem. Biophys. Res. Commun.* **167**, 89–95 (1990).
33. R. R. Montgomery, D. Lusitani, A. de Boisfleury Chevance, S. E. Malawista, Human phagocytic cells in the early innate immune response to Borrelia burgdorferi. *J. Infect. Dis.* **185**, 1773–1779 (2002).
34. J. T. Park, T. Uehara, How bacteria consume their own exoskeletons (turnover and recycling of cell wall peptidoglycan). *Microbiol. Mol. Biol. Rev.* **72**, 211–227 (2008).
35. E. W. Goodell, U. Schwarz, Release of cell wall peptides into culture medium by exponentially growing Escherichia coli. *J. Bacteriol.* **162**, 391–397 (1985).
36. C. Jacobs, L. J. Huang, E. Bartowsky, S. Normark, J. T. Park, Bacterial cell wall recycling provides cytosolic muropeptides as effectors for beta-lactamase induction. *EMBO J.* **13**, 4684–4694 (1994).
37. D. M. Adin, J. T. Engle, W. E. Goldman, M. J. McFall-Ngai, E. V. Stabb, Mutations in ampG and lytic transglycosylase genes affect the net release of peptidoglycan monomers from Vibrio fischeri. *J. Bacteriol.* **191**, 2012–2022 (2009).
38. G. Nigro *et al*., Muramylpeptide shedding modulates cell sensing of Shigella flexneri. *Cell. Microbiol.* **10**, 682–695 (2008).
39. D. L. Garcia, J. P. Dillard, Mutations in ampG or ampD affect peptidoglycan fragment release from Neisseria gonorrhoeae. *J. Bacteriol.* **190**, 3799–3807 (2008).
40. S. C. Holt, Anatomy and chemistry of spirochetes. *Microbiol. Rev.* **42**, 114–160 (1978).
41. K. H. Schleifer, R. Joseph, A directly cross-linked L-ornithine-containing peptidoglycan in cell walls of Spirochaeta stenostrepta. *FEBS Lett.* **36**, 83–86 (1973).
42. S. E. Girardin *et al*., Nod2 is a general sensor of peptidoglycan through muramyl dipeptide (MDP) detection. *J. Biol. Chem.* **278**, 8869–8872 (2003).
43. J. T. Tigno-Aranjuez, J. M. Asara, D. W. Abbott, Inhibition of RIP2's tyrosine kinase activity limits NOD2-driven cytokine responses. *Genes Dev.* **24**, 2666–2677 (2010).
44. S. E. Girardin *et al*., Peptidoglycan molecular requirements allowing detection by Nod1 and Nod2. *J. Biol. Chem.* **278**, 41702–41708 (2003).
45. H. A. Verbrugh, R. Peters, M. Rozenberg-Arska, P. K. Peterson, J. Verhoef, Antibodies to cell wall peptidoglycan of Staphylococcus aureus in patients with serious staphylococcal infections. *J. Infect. Dis.* **144**, 1–9 (1981).
46. H. I. Wergeland, C. Endresen, Antibodies to various bacterial cell wall peptidoglycans in human and rabbit sera. *J. Clin. Microbiol.* **25**, 540–545 (1987).
47. P. M. Johnson, K. K. Phua, H. R. Perkins, C. A. Hart, R. C. Bucknall, Antibody to streptococcal cell wall peptidoglycan-polysaccharide polymers in seropositive and seronegative rheumatic disease. *Clin. Exp. Immunol.* **55**, 115–124 (1984).
48. Y. Todome *et al*., Detection of antibodies against streptococcal peptidoglycan and the peptide subunit (synthetic tetra-D-alanyl-bovine serum albumin complex) in rheumatic-diseases. *Int. Arch. Allergy Immunol.* **97**, 301–307 (1992).
49. J. J. Shin, L. J. Glickstein, A. C. Steere, High levels of inflammatory chemokines and cytokines in joint fluid and synovial tissue throughout the course of antibiotic-refractory Lyme arthritis. *Arthritis Rheum.* **56**, 1325–1335 (2007).
50. R. B. Lochhead *et al*., Robust interferon signature and suppressed tissue repair gene expression in synovial tissue from patients with postinfectious, Borrelia burgdorferi-induced Lyme arthritis. *Cell. Microbiol.* **21**, e12954 (2019).
51. K. N. Couper, D. G. Blount, E. M. Riley, IL-10: The master regulator of immunity to infection. *J. Immunol.* **180**, 5771–5777 (2008).
52. A. A. Belperron, N. Liu, C. J. Booth, L. K. Bockenstedt, Dual role for Fcγ receptors in host defense and disease in Borrelia burgdorferi-infected mice. *Front. Cell. Infect. Microbiol.* **4**, 75 (2014).
53. A. A. Belperron, C. M. Dailey, C. J. Booth, L. K. Bockenstedt, Marginal zone B-cell depletion impairs murine host defense against Borrelia burgdorferi infection. *Infect. Immun.* **75**, 3354–3360 (2007).
54. J. Royet, R. Dziarski, Peptidoglycan recognition proteins: Pleiotropic sensors and effectors of antimicrobial defences. *Nat. Rev. Microbiol.* **5**, 264–277 (2007).
55. T. Kawai, S. Akira, Toll-like receptors and their crosstalk with other innate receptors in infection and immunity. *Immunity* **34**, 637–650 (2011).
56. I. G. Boneca, The role of peptidoglycan in pathogenesis. *Curr. Opin. Microbiol.* **8**, 46–53 (2005).
57. S. K. Singh, H. J. Girschick, Lyme borreliosis: From infection to autoimmunity. *Clin. Microbiol. Infect.* **10**, 598–614 (2004).
58. K. Strle, J. J. Shin, L. J. Glickstein, A. C. Steere, Association of a toll-like receptor 1 polymorphism with heightened Th1 inflammatory responses and antibiotic-refractory Lyme arthritis. *Arthritis Rheum.* **64**, 1497–1507 (2012).
59. R. B. Lochhead *et al*., Interferon-gamma production in Lyme arthritis synovial tissue promotes differentiation of fibroblast-like synoviocytes into immune effector cells. *Cell. Microbiol.* **21**, e12992 (2019).
60. F. G. Dalldorf, W. J. Cromartie, S. K. Anderle, R. L. Clark, J. H. Schwab, The relation of experimental arthritis to the distribution of streptococcal cell wall fragments. *Am. J. Pathol.* **100**, 383–402 (1980).
61. S. N. Lichtman *et al*., Bacterial cell wall polymers (peptidoglycan-polysaccharide) cause reactivation of arthritis. *Infect. Immun.* **61**, 4645–4653 (1993).
62. M. J. Melief, M. A. Hoijer, H. C. Van Paassen, M. P. Hazenberg, Presence of bacterial flora-derived antigen in synovial tissue macrophages and dendritic cells. *Br. J. Rheumatol.* **34**, 1112–1116 (1995).
63. J. Malda, J. Boere, C. H. van de Lest, P. van Weeren, M. H. Wauben, Extracellular vesicles—New tool for joint repair and regeneration. *Nat. Rev. Rheumatol.* **12**, 243–249 (2016).
64. I. A. Schrijver *et al*., Peptidoglycan from sterile human spleen induces T-cell proliferation and inflammatory mediators in rheumatoid arthritis patients and healthy subjects. *Rheumatology* **40**, 438–446 (2001).
65. I. A. Schrijver, M. J. Melief, P. P. Tak, M. P. Hazenberg, J. D. Laman, Antigen-presenting cells containing bacterial peptidoglycan in synovial tissues of rheumatoid arthritis patients coexpress costimulatory molecules and cytokines. *Arthritis Rheum.* **43**, 2160–2168 (2000).
66. D. Sun *et al*., Bacillus anthracis peptidoglycan activates human platelets through FcγRII and complement. *Blood* **122**, 571–579 (2013).
67. Y. E. Johnston *et al*., Lyme arthritis. Spirochetes found in synovial microangiopathic lesions. *Am. J. Pathol.* **118**, 26–34 (1985).
68. D. Londoño *et al*., Antibodies to endothelial cell growth factor and obliterative microvascular lesions in the synovium of patients with antibiotic-refractory Lyme arthritis. *Arthritis Rheumatol.* **66**, 2124–2133 (2014).
69. J. A. Hardin, A. C. Steere, S. E. Malawista, Immune complexes and the evolution of Lyme arthritis. Dissemination and localization of abnormal C1q binding activity. *N. Engl. J. Med.* **301**, 1358–1363 (1979).
70. D. L. Greenway, H. R. Perkins, Turnover of the cell wall peptidoglycan during growth of Neisseria gonorrhoeae and Escherichia coli. Relative stability of newly synthesized material. *J. Gen. Microbiol.* **131**, 253–263 (1985).
71. R. S. Rosenthal, Release of soluble peptidoglycan from growing gonococci: Hexaminidase and amidase activities. *Infect. Immun.* **24**, 869–878 (1979).

72. M. A. Melly, Z. A. McGee, R. S. Rosenthal, Ability of monomeric peptidoglycan fragments from Neisseria gonorrhoeae to damage human fallopian-tube mucosa. *J. Infect. Dis.* **149**, 378–386 (1984).
73. M. V. Norgard, B. S. Riley, J. A. Richardson, J. D. Radolf, Dermal inflammation elicited by synthetic analogs of Treponema pallidum and Borrelia burgdorferi lipoproteins. *Infect. Immun.* **63**, 1507–1515 (1995).
74. K. B. Gondolf, M. Mihatsch, E. Curschellas, J. J. Dunn, S. R. Batsford, Induction of experimental allergic arthritis with outer surface proteins of Borrelia burgdorferi. *Arthritis Rheum.* **37**, 1070–1077 (1994).
75. S. Batsford, J. Dunn, M. Mihatsch, Outer surface lipoproteins of Borrelia burgdorferi vary in their ability to induce experimental joint injury. *Arthritis Rheum.* **50**, 2360–2369 (2004).
76. N. W. Schröder *et al*., Acylated cholesteryl galactoside as a novel immunogenic motif in Borrelia burgdorferi sensu stricto. *J. Biol. Chem.* **278**, 33645–33653 (2003).
77. V. Pozsgay *et al*., Synthesis and antigenicity of BBGL-2 glycolipids of Borrelia burgdorferi, the causative agent of Lyme disease. *Carbohydr. Res.* **346**, 1551–1563 (2011).
78. A. G. Barbour, Isolation and cultivation of Lyme disease spirochetes. *Yale J. Biol. Med.* **57**, 521–525 (1984).
79. B. L. Jutras *et al*., Lyme disease and relapsing fever Borrelia elongate through zones of peptidoglycan synthesis that mark division sites of daughter cells. *Proc. Natl. Acad. Sci. U.S.A.* **113**, 9162–9170 (2016).
80. B. Glauner, Separation and quantification of muropeptides with high-performance liquid chromatography. *Anal. Biochem.* **172**, 451–464 (1988).
81. A. Gründling, O. Schneewind, Cross-linked peptidoglycan mediates lysostaphin binding to the cell wall envelope of Staphylococcus aureus. *J. Bacteriol.* **188**, 2463–2472 (2006).
82. M. Tsuchiya, N. Asahi, F. Suzuoki, M. Ashida, S. Matsuura, Detection of peptidoglycan and beta-glucan with silkworm larvae plasma test. *FEMS Immunol. Med. Microbiol.* **15**, 129–134 (1996).
83. N. K. Bui *et al*., The peptidoglycan sacculus of Myxococcus xanthus has unusual structural features and is degraded during glycerol-induced myxospore development. *J. Bacteriol.* **191**, 494–505 (2009).
84. P. Schumann, Peptidoglycan structure. *Methods Microbiol.* **38**, 101–129 (2011).
85. B. L. Jutras, A. M. Chenail, B. Stevenson, Changes in bacterial growth rate govern expression of the Borrelia burgdorferi OspC and Erp infection-associated surface proteins. *J. Bacteriol.* **195**, 757–764 (2013).
86. D. Molnár, G. Soltész, J. Mestyán, The metabolic effects of cold exposure in the newborn rabbit. *Biol. Neonate* **36**, 215–219 (1979).
87. M. Wharton, T. L. Chorba, R. L. Vogt, D. L. Morse, J. W. Buehler, Case definitions for public health surveillance. *MMWR Recomm. Rep.* **39**, 1–43 (1990).
88. G. P. Wormser *et al*., The clinical assessment, treatment, and prevention of lyme disease, human granulocytic anaplasmosis, and babesiosis: Clinical practice guidelines by the Infectious Diseases Society of America. *Clin. Infect. Dis.* **43**, 1089–1134 (2006).
89. D. Aletaha *et al*., 2010 rheumatoid arthritis classification criteria: An American College of Rheumatology/European League Against Rheumatism collaborative initiative. *Arthritis Rheum.* **62**, 2569–2581 (2010).
90. D. Veale, S. Rogers, O. Fitzgerald, Classification of clinical subsets in psoriatic arthritis. *Br. J. Rheumatol.* **33**, 133–138 (1994).
91. R. Altman *et al*.; Diagnostic and Therapeutic Criteria Committee of the American Rheumatism Association Development of criteria for the classification and reporting of osteoarthritis. Classification of osteoarthritis of the knee. *Arthritis Rheum.* **29**, 1039–1049 (1986).
92. R. B. Lochhead *et al*., MicroRNA expression shows inflammatory dysregulation and tumor-like proliferative responses in joints of patients with postinfectious Lyme arthritis. *Arthritis Rheumatol.* **69**, 1100–1110 (2017).
93. R. R. Montgomery *et al*., Recruitment of macrophages and polymorphonuclear leukocytes in Lyme carditis. *Infect. Immun.* **75**, 613–620 (2007).